Received:

Revised:

Accepted:

Published:

Solving Wound Perimeter Detection with Active Contour Model Enhanced with Interpolation

Muhammad Eka Suryana [1, a)], Muhammad Rizki [1, b)], Med Irzal [1, c)], Ratna Aryani [2, d)]

Author Affiliations
[1](*Computer Science Programme, Faculty of Mathematic & Science, Universitas Negeri Jakarta, Jakarta, Indonesia*)
[2](*Nursery Department*, *Politeknik Kesehatan Jakarta 1, Jakarta, Indonesia*).

Author Emails
a) eka-suryana@unj.ac.id
b) muhammadrizki109@gmail.com
c) medirzal@unj.ac.id
d) ratna_aryani@poltekkesjakarta1.ac.id
Corresponding author: eka-suryana@unj.ac.id

Abstract. Active Contour Model is the most original algorithm among the class of Contour Finding methods. Its capability is tested against wound parameter detection given an image data. The performance is less satisfying, in general few perimeter are found correctly but the rest are far from ideal. However, through some tuning by adding an extra pre-processing step the result can be improved. Image Interpolation is used to achieve this improvement. This paper reports how significant the improvement ae.

I. Introduction

Active Contour Model is the method to find the contour of an image, this method was first introduced by Kass et.al in 1988 (1). Contour is considered as higher level features than edge. Fundamentally, Active Contour is a curve which minimize energy function based on surrounding information. This energy is composed of two functions: internal energy which controlled the smoothness and tautness of the curve and external energy which pull the curve toward feature of interest (2). Original Active Contour has two weaknesses in accuracy of final curve obtained depend on the distance between initial curve with feature of interest, in our case wound perimeter. The further the initial curve from the perimeter, the worsen final curve result will be. Secondly, active contour is unable closing to region near the concave boundary (3), (4). Due to this property, some bio-medical problems are unable to be solved with Active Contour. In 2016 however, Abdullah et.al in Bio-Medical problem proposed a variation of Active Contour on Iris Segmentation. He changed the external energy of Active Contour to *pressure force* such that the curve moved closer to the eyelid accurately (5). In our case, we applied Active Contour to chronic wound perimeter detection. Just like the previous case, Active Contour test result is less satisfying. Therefore an extra preprocessing stage is added to the original image such that the result been improved. The rest of the paper explain technical details of the step. But first before the details be further elaborated, review of recent trends in wound medical imaging will be given in this section.

The research focus in wound medical imaging can be broken down into several directions. Wang et.al. In 2016 tried to solved similar problem in wound boundary detection. His solution consists of several stages of processing, it initially started with SLIC segmentation as pre-stage. Then in the first stage, k-binary SVM classifier is run on the superpixedl. In the second stage, incorrectly classified set is trained upon another binary SVM classifier. Second stage resulting in color & texture information which later transformed as local dense scale invariant feature descriptors. This descriptor is a feature which defined the wound boundary (6). The result shown much improvement compared to his earlier research which conduct similar research but accomplished with mean shift (7).

In wound size finding, White et.al. Proposed 3 theoretical concepts which brought feasibility to compute wound size automatically. These are 1). depth finding from camera autofocus 2). Sensor fusion from Magnetometer, Gyroscope, Accelerometer combined with internal feature tracking on camera 3). Pinch/zoom with known reference size. Out of these three, pinch/zoom was the most accurate & feasible, therefore developed into full prototype (8). Since White et.al. needs feature tracking data from camera data, Poon et.al conduct similar research but without this necessity. He replaced it with Grab Cut for tracking wound object, whereas for wound size determination he basically used similar approach with White et. al. Through Pinch & zoom method with known reference point with extra processing to project 3d camera capture to 2d plane. Not only on wound size finding, Poon also contributed in color image analysis through Red, Green, Blue histogram similarity (9).

Some researches are focused on color segmentation of the wound. Wang. et.al. Proposed wound boundary detection with mean-shift based algorithm continued with k-means clustering to colorize the wound into red, yellow, black colors (10). Previously, Poucke et. al. conducts automatic colorimetric calibration of wounds. Motivation of his research was due to various camera equipment which lead to the resulting slightly different colors of the final image. Post calibration the wounds image was to be stored in sRGB color space. Although this research is produced complicated method just to calibrating wound colors, but it would be prospective if integrated into camera hardware (11). Li et. al. complained progress in wound segmentation reseach burdened by manual feature extractions. Thus, he proposed deep learning based automatic wound segmentation. One limitation of deep learning model is the necessities for the manually labeled ground truth data. Li avoided this pitfall by generating location based information which the model was trained upon (12).

We are interested to conduct similar researches in wound boundary detection using Active Parametric Contour, due to the resulting success when the method was applied for iris perimeter finding (5).

II. Methodology

Let's defined $\boldsymbol{u}$ as a a curve which the active parametric contour that will converge at the end. It stored the curve in x & y coordinates respectively. Whereas s is the index of the curve at the given query position (13).

$$u(s)=(x(s),y(s)) \tag{1}$$

In order to learn, the curve has to be defined as a function. This function will be minimized with respect to $x(s)$ and $y(s)$. External energy is the one responsible which moved the curve to location of interest, while internal energy served limit the curve movement according to stiffness or elasticity.

$$E(X,Y)=E_{internal}(X,Y)+E_{external}(X,Y) \tag{2}$$

Formally let's define the internal energy as

$$E_{internal}(X,Y)=\frac{1}{2}\int_0^1 \alpha\left[\left|\frac{dX}{ds}\right|^2+\left|\frac{dY}{ds}\right|^2\right]+\beta\left[\left|\frac{d^2X}{ds^2}\right|^2+\left|\frac{d^2Y}{ds^2}\right|^2\right]ds \tag{3}$$

Which α, β are parameters which control elasticity and stiffness respectively. Moving on, external energy is defined as

$$E_{external}(X,Y)=-\int_0^1 f(X(s),Y(s))ds \tag{4}$$

Equation (4) seems a recursive of equation (2) since it delved deeper into more function. Here we need to replace *f* with a function which represented the image. Therefore its called external due to the function conjugate with external surrounding of the curve whereas internal is due to the function represent the curve itself.

Xu suggest using Gaussian function to represent external energy (14). Correspondingly, Gaussian function when applied on the image gives smoothing to the whole area. Minimizing this function is estimated to reverse it, which moved the curve to the nearest contour. In definite form the function is represented as

$$E_{external}(X,Y)=-\left|\nabla[G_\sigma(x,y)*I(x,y)]\right|^2 \tag{5}$$

We want to minimize equation (2), it can be done by setting the right set of the equation to 0 then derive the all symbols with regards to time. Mathematically speaking, this can be achieved with Newton method, however for computation feasibility sake gradient descent is more appropriate. Xu has simplified the application of gradient descent in equation (2) such that the final form can be written into the following formulas

$$\mathbf{M}=\begin{bmatrix} r & q & p & & & p & q \\ q & r & q & p & & & p \\ p & q & r & q & p & & \\ & \ddots & \ddots & \ddots & \ddots & \ddots & \\ & & p & q & r & q & p \\ p & & & p & q & r & q \\ q & p & & & p & q & r \end{bmatrix} \tag{6}$$

M is a Matrix which represent the curve internal energy. Final update equation which iterate the curve until it converge laid in equation (9). The curve is updated per iteration by multiplicating inverse of *M* with the added sum of between current curve and derivative of external energy. Derivation of external energy in equation (5) is simply image gradient.

$$\tilde{\mathbf{u}}_j^{t+1} = \begin{bmatrix} \tilde{u}_0^{t+1} \\ \tilde{u}_1^{t+1} \\ \tilde{u}_2^{t+1} \\ \vdots \\ \tilde{u}_{N-3}^{t+1} \\ \tilde{u}_{N-2}^{t+1} \\ \tilde{u}_{N-1}^{t+1} \end{bmatrix} = \begin{bmatrix} u_0^t + \delta t \frac{\partial E_{ext}^{(i)}}{\partial u_0^t} \\ u_1^t + \delta t \frac{\partial E_{ext}^{(i)}}{\partial u_1^t} \\ u_2^t + \delta t \frac{\partial E_{ext}^{(i)}}{\partial u_2^t} \\ \vdots \\ u_{N-3}^t + \delta t \frac{\partial E_{ext}^{(i)}}{\partial u_{N-3}^t} \\ u_{N-2}^t + \delta t \frac{\partial E_{ext}^{(i)}}{\partial u_{N-2}^t} \\ u_{N-1}^t + \delta t \frac{\partial E_{ext}^{(i)}}{\partial u_{N-1}^t} \end{bmatrix} \tag{7}$$

$$p \equiv \beta \frac{\delta t}{\delta s^4}, q \equiv -\alpha \frac{\delta t}{\delta s^2} - 4\beta \frac{\delta t}{\delta s^4}, r \equiv 1 + 2\alpha \frac{\delta t}{\delta s^2} + 6\beta \frac{\delta t}{\delta s^4} \tag{8}$$

$$\mathbf{u}_j^{t+1} = \mathbf{M}^{-1} \left(\mathbf{u}_j^t + \delta t \frac{\partial E_{ext}^{(i)}}{\partial \mathbf{u}_j^t} \right) \tag{9}$$

III. Experiment Schemes

For the experiment data consisting of 108 wound images were taken during the clinical trials of chronic wound treatments on Nursery Department on Politeknik Kesehatan Jakarta 1 back on 2018. Not all entries are acceptable, therefore 37 images were discarded. Of the remainder data, black chronic wound images were numbering in 32 entries. Red wound images were accumulating in similarly 32 entries. Yellow wound images were the most smaller amount to only 15 images. These data set then manually border annotated by experts using GIMP software. Example of an entry is shown next in Figure 1.

Figure 1: Instance of Wound Data Set: left - RGB image, middle - ground truth from expert, right - processed ground truth

For result comparison, processed ground truth after applied with edge detection will be used. While the input images are in RGB color space, parametric active contour which would be applied into it only runnable on single channel color. The following Figure 2 shows the process until initial curve is made. Initial curve needs to be fit inside the skin region, if the initial curve broken past this restriction. The resulting converged curve will worsen such as shown on Figure 3.

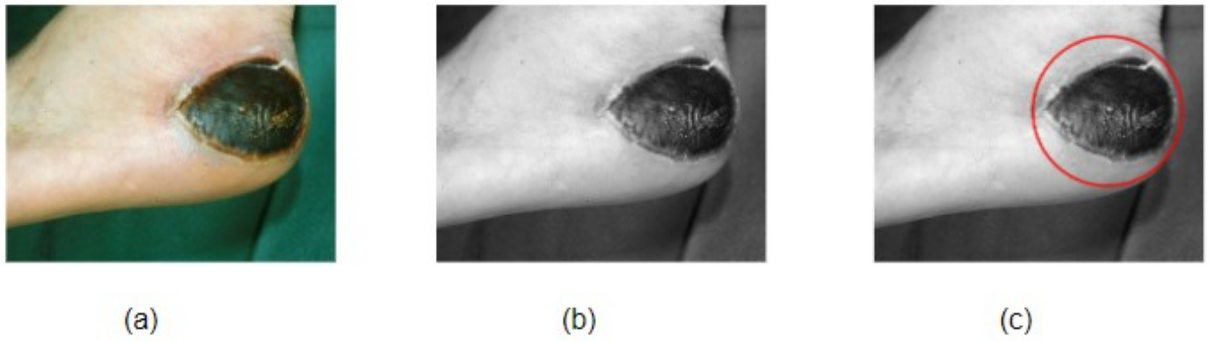

Figure 2: Image Transformation: (a) untouched, (b) Grayscale transformation, (c) initially made curve

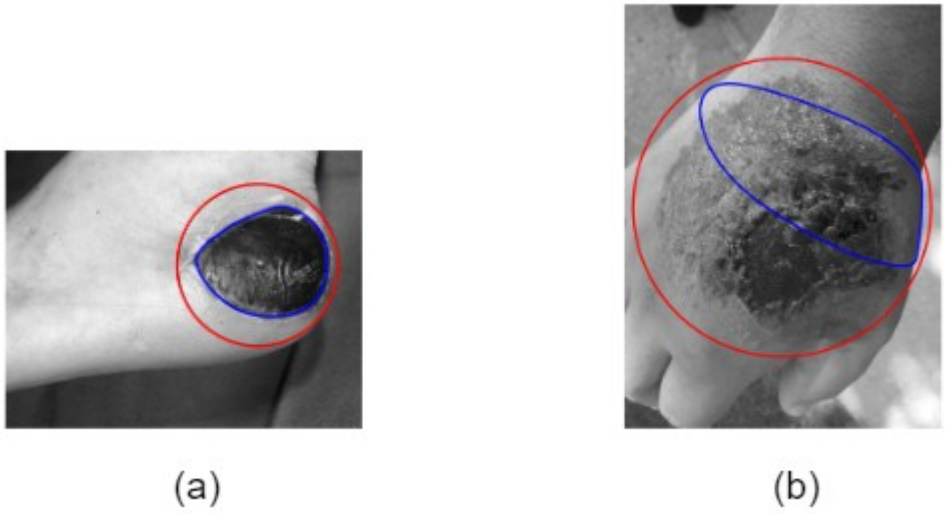

Figure 3: Sample Final Curves: (a) good finding. (b) bad finding

Quantitatively, comparison between produced curve with the ground truth need to be computed. We can do this by finding the area difference between ground truth with the final curve. The result is shown on Figure 4.

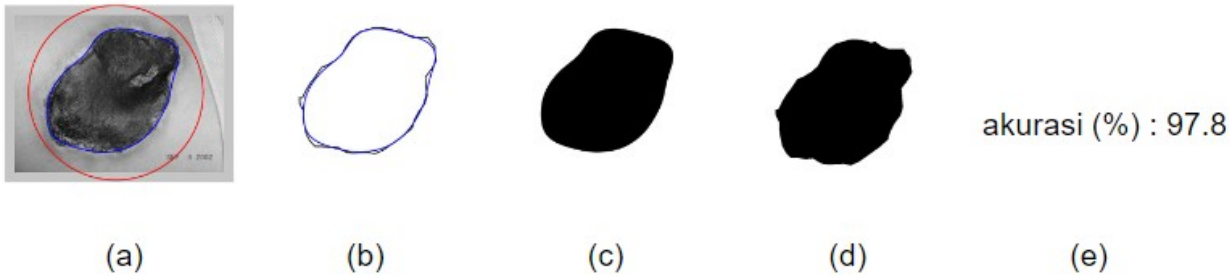

Figure 4: Compared Result. Focus on comparison between (c) & (d) along with its quantitative value (e).

Generally Active Contour has less satisfying results when applied on Wound Images. The figure 5 shown an instance result which failed to converge to proper wound perimeter (a). In comparison after applying image interpolation the curve converged better (b). Green lines are showing the update to the curve per iteration.

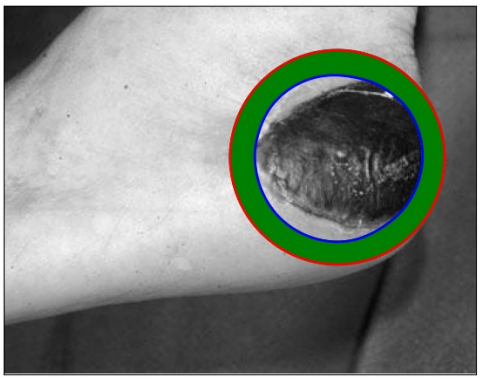

(a) Active Contour on the Original Image

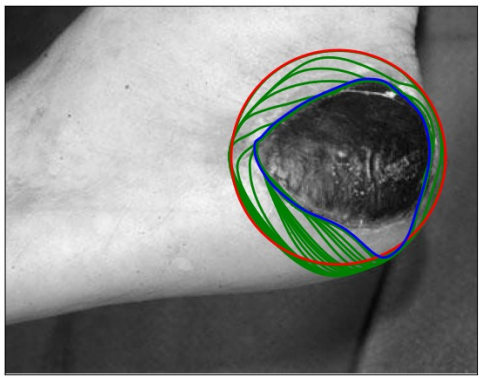

(b) Active Contour on Interpolated Image

Figure 5: Active Contour Results

IV. Result Analysis

In Figure 5, we are presented with active contour and its comparison with pre-applied interpolation. If the underlying theory presented in chapter 2 is correct, it should converge with the similar result. To answer this doubt, let us review the final update curve on equation 9. u is a curve which computationally speaking represented as consecutive points that started at initial point and ended at last point. In wound case the curve must be closed, starting and last point intersect. Here we encounter miss match between original curve definition which is continuous on equation 1 with real data that represented as discrete points. The higher resolution the image, the better discrete points will be sampled. In contrast, for low resolution image there will be jagged curve due to steep jump between points. The matter becomes more complicated due to equation 9 which updated the curve position. Intial curve is stored in pair of x, y coordinates, and we knew that coordinates have to be integer. Due to the update equation which involved matrix inversion, multiplication with floating values and image gradient. Just after an update, the curve is hardly integer. In active contour the coordinate is used to query external images values, which have to be integer. In case of this, rounding is performed. This seemingly trivial operation, alter the result such that in got stuck in certain position such as shown in Figure 5. Thus, this was one of the reason Active Contour perform better on higher resolution image, since higher sampling provides approximately continuous values.

Interpolation behaves differently if ran on the image. Usually, it will extrapolate samples such that the curve is smoothed out. This behavior produced more samples which can be controlled by stepping factor of interpolation. However interpolation in image need to produced same dimension. Secondly basic interpolation support one dimensional where as image are two dimensions. Thus interpolation in this domain, involved heavier computations. Image interpolation can be done implicitly or explicitly. Explicit interpolation will produced intermediate larger image size which will be downsized to the original resolution. In contrast implicit interpolation do the same thin though approximate function. Both have trade offs but ultimately it resulted in sharpening the contrast of the image instead of curve smoothing that produced in typical interpolation. See how interpolated image produced more clear contour in Figure 6.

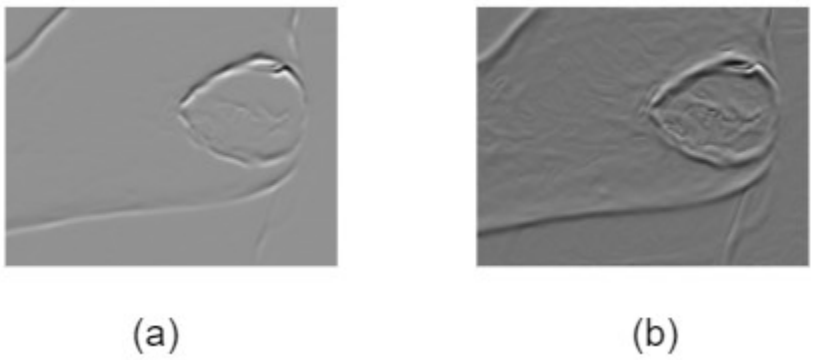

Figure 6: Image Interpolation: a) lower manifold of original image b) lower manifold of interpolated image

V. CONCLUSION

In general, we can expect Parametric Active Contour to perform better when the image is pre-processed with Interpolation. Although the significance is varying case by case. With parametric active contour we can hardly expect the curve to be fit in the same location as the ground truth, although the converged curve will sit near the ground truth lines. This near but different wound boundary parameter need to be evaluated with health expert.

REFERENCES

1. Kass, M., Witkin, A., and Terzopoulos, D. Snakes: Active contour models. International journal of computer vision, 1(4):321–331 (1988).
2. Acton, S. and Ray, N. . Biomedical image analysis: Segmentation (synthesis lectures on image, video, & multimedia processing). (Morgan & Claypool Publishers, 2007), pp3-37.
3. Xu, C. and Prince, J. L. Snakes, shapes, and gradient vector flow. IEEE Transactions on image processing, 7(3):359–369 (1998)
4. Guo, M., Wang, Z., Ma, Y., and Xie, W. Review of parametric active contour models in image processing. Journal of Convergence Information Technology, 8(11):248 (2013).
5. Abdullah, M. A., Dlay, S. S., Woo, W. L., and Chambers, J. A. Robust iris segmentation method based on a new active contour force with a noncircular normalization. IEEE transactions on systems, man, and cybernetics: Systems, 47(12):3128–3141 (2016).
6. Wang, L., Pedersen, P. C., Agu, E., Strong, D. M., and Tulu, B. Area determination of diabetic foot ulcer images using a cascaded two-stage svm-based classification. IEEE Transactions on Biomedical Engineering, 64(9):2098–2109 (2016).
7. Wang, L., Pedersen, P. C., Strong, D. M., Tulu, B., Agu, E., and Ignotz, R. Smartphone-based wound assessment system for patients with diabetes. IEEE Transactions on Biomedical Engineering, 62(2):477–488. (2014).
8. White, P. J., Podaima, B. W., and Friesen, M. R. (2014). Algorithms for smartphone and tablet image analysis for healthcare applications. IEEE Access, 2:831–840.
9. Poon, T. W. K. and Friesen, M. R. Algorithms for size and color detection of smartphone images of chronic wounds for healthcare applications. IEEE Access, 3:1799–1808. (2015).

10. Wang, L., Pedersen, P. C., Strong, D. M., Tulu, B., Agu, E., and Ignotz, R. Smartphone-based wound assessment system for patients with diabetes. IEEE Transactions on Biomedical Engineering, 62(2):477–488. (2014).
11. Van Poucke, S., Vander Haeghen, Y., Vissers, K., Meert, T., and Jorens, P. Automatic colorimetric calibration of human wounds. BMC medical imaging, 10(1):7. (2010).
12. F. Li, C. Wang, Y. Peng, Y. Yuan and S. Jin, "Wound Segmentation Network Based on Location Information Enhancement," in *IEEE Access*, vol. 7, pp. 87223-87232, 2019, doi: 10.1109/ACCESS.2019.2925689.
13. Acton, S. and Ray, N. (2007). Biomedical image analysis: Segmentation (synthesis lectures on image, video, & multimedia processing). Morgan & Claypool Publishers.
14. Xu, C. and Prince, J. L. Snakes, shapes, and gradient vector flow. IEEE Transactions on image processing, 7(3):359–369. (1998).
15. Abdullah, M. A., Dlay, S. S., Woo, W. L., and Chambers, J. A. Robust iris segmentation method based on a new active contour force with a noncircular normalization. IEEE transactions on systems, man, and cybernetics: Systems, 47(12):3128–3141. (2016).